JCTC Journal of Chemical Theory and Computation

Article

pubs.acs.org/JCTC

Adsorption of Water onto $SrTiO_3$ from Periodic Møller–Plesset Second-Order Perturbation Theory

E. Holmström*[,†] and A. S. Foster[†,‡]

[†]COMP, School of Science, Aalto University, P.O. Box 11100, FI-00076 Aalto, Finland

[‡]Division of Electrical Engineering and Computer Science, Kanazawa University, Kanazawa 920-1192, Japan

ABSTRACT: Adsorption of water onto metal oxide surfaces is a long-standing problem motivated by relevance to many promising technological applications. In this work, we compute the adsorption energy of water on $SrTiO_3$ using periodic Møller–Plesset second-order perturbation theory (MP2). We compare our MP2 results to density functional and hybrid density functional theory calculations with and without the widely used D3 dispersion correction. The MP2 ground-state adsorption energy of water on $SrTiO_3$ (001) at one monolayer coverage is 0.9 eV on the TiO_2 termination in the molecular configuration and 0.6 eV in the dissociative configuration, the corresponding results on the SrO termination being 0.9 eV for both modes of adsorption. These results are reproduced well by the PBE and PBE0 exchange-correlation functionals. Correcting for dispersion effects through the D3 dispersion correction leads to significantly overestimated adsorption energies for both PBE and PBE0 with respect to MP2. The D3 correction also fails to capture the difference in electron correlation between the molecular and dissociative adsorption states, similarly to the optB86b van der Waals density functional.

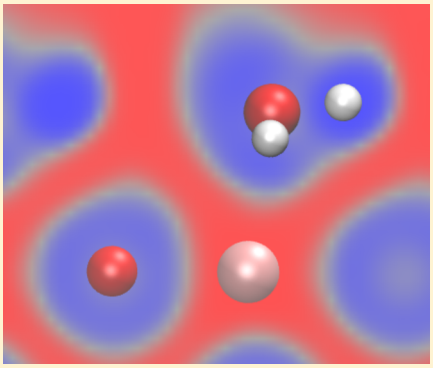

INTRODUCTION

The interaction of water and metal oxide surfaces is a long-standing theoretical challenge, motivated largely by the great technological potential of photocatalytic metal oxides in heterogeneous catalysis[1−4] and the ubiquity of solid–liquid interfaces of metal oxides and water.[5,6] A large body of research has been dedicated to using density functional theory (DFT) to model the adsorption of water onto metal oxides of photocatalytical capability, such as TiO_2[7−11] and $SrTiO_3$.[12−16] Recently, however, attention has been drawn to the fact that results of such calculations, performed mostly in static conditions through geometry optimization, depend sensitively on the choice of exchange-correlation functional, the treatment of the dispersion interaction, and other factors, such as a possible Hubbard term for d–d electron interaction. Large variation in the energy of water adsorption at a fixed level of coverage with these parameters has been documented for TiO_2[17] and is apparent in results for $SrTiO_3$ as well.[16] The variation exists even in the case that finite-size effects arising from the thickness of the slab used to model the crystal surface are eliminated.[17,18] While good qualitative agreement between DFT results and observation has been achieved with respect to the favored state of adsorbed water (molecular or dissociated) as a function of water coverage on some metal oxide surfaces,[14] overall it appears that DFT in its current state is not able to give a quantitatively reliable description of the adsorption of water onto metal oxides. It is therefore necessary to use higher-level quantum-mechanical methods in the treatment of the problem. To date, Møller–Plesset second-order perturbation theory (MP2) has been applied to treat water on MgO[19] and TiO_2[20] and other metal oxides,[21] and coupled-cluster calculations have been performed for water on TiO_2,[22] with the crystal being treated in all of these studies through a nonperiodic cluster geometry.

In this work, we use periodic MP2 theory to model the adsorption of water onto the planar surface of the prototypical metal oxide photocatalyst $SrTiO_3$. For comparison with our MP2 results, we compute the adsorption energy of water on the (001) surface of the crystal for both the SrO and the TiO_2 terminations using a hierarchy of methods at the DFT, van der Waals DFT, hybrid-functional DFT, and Hartree–Fock level, and we also consider the effect of dispersion correction on the DFT and hybrid functional DFT approaches. Our MP2 results provide a standard against which to gauge existing and future models of the adsorption of water onto this widely considered metal oxide and related materials. Furthermore, our results allow us to probe the role of electron correlation in the adsorption process, as well as to directly assess the accuracy of the employed range of methods with respect to MP2.

METHODS

Our objective is to compute the static adsorption energy of water on $SrTiO_3$ as accurately as possible and to assess the accuracy of commonly used approaches to the problem. To accomplish this, we treat the electronic structure of our model system using a range of methods: pure DFT and hybrid-functional DFT, these two augmented with a postcorrection to

Received: May 31, 2017
Published: November 7, 2017

DOI: 10.1021/acs.jctc.7b00549
J. Chem. Theory Comput. 2017, 13, 6301−6307

account for the dispersion interaction, DFT using a van der Waals exchange-correlation functional, Hartree−Fock, and MP2. Using each method, we first find the equilibrium lattice constant, bulk modulus, and band gap of the $SrTiO_3$ crystal. Then, we find the adsorption energy of water onto the $SrTiO_3$ surface through separately computing the energy of the isolated water molecule, the periodic slab in vacuum, and the energy of the slab system with the water molecule adsorbed onto the surface. We use the VASP[23−25] code for all our electronic structure calculations, through which we employ a plane wave basis set in a periodic supercell using the projector-augmented wave method.[24,26]

To model exchange and correlation in our pure DFT approach, we choose the widely used generalized-gradient-approximation (GGA) level PBE functional.[27] We use a kinetic cutoff energy of E_{cut} = 550 eV for the plane wave basis set in all our DFT, hybrid-functional DFT, van der Waals DFT, and Hartree−Fock calculations (except Hartree−Fock within the MP2 method, see below). Our test calculations indicate that using a 6 × 6 × 6 Monkhorst−Pack[28] grid of k-points to sample the first Brillouin zone gives total energies converged to within 5 meV per unit of $SrTiO_3$ for the bulk crystal. For the H_2O molecule in vacuum, using a cubic supercell of size 20 Å × 20 Å × 20 Å gives an energy converged to within 10 meV, whereas a k-point grid of 6 × 6 × 1 gives a convergence of energy to within 20 meV for the total slab and molecule system. We use these k-point grids for all our PBE calculations.

To represent the hybrid functional approach, we choose the PBE0 functional.[29,30] Our test calculations indicate that a slightly denser grid of k-points is necessary to obtain a well-converged total energy for PBE0 than it is for PBE. For the bulk crystal, 8 × 8 × 8 k-points is necessary to obtain convergence to within 10 meV per unit of $SrTiO_3$, whereas a cubic supercell of 20 Å × 20 Å × 20 Å gives an energy converged to within 10 meV for the single H_2O molecule. An 8 × 8 × 1 k-point grid gives energies converged to within 40 meV for the total slab and molecule system. These are the parameters we use for all our PBE0 calculations. To account for the dispersion interaction[31] in our DFT simulations, we use the optB86b van der Waals functional,[32−35] using the same k-point sampling as for the hybrid functional calculations. In addition, we augment our PBE and PBE0 functionals with the Grimme D3 dispersion correction,[36] as parametrized separately for each functional.[37]

The total MP2 energy of a system of electrons and nuclei is equal to the sum of the Hartree−Fock energy and the MP2 correlation energy, i.e., $E_{MP2} = E_{HF} + E_{MP2}^{corr}$.[38] We compute E_{HF} for each system using the same k-point sampling as in our PBE0 calculations. Then, we compute the MP2 correlation energy E_{MP2}^{corr} for a given system in two stages. To make the calculation feasible for the extended systems involving the crystal slab, we decrease the plane wave cutoff energy to 400 eV. First, we find the Hartree−Fock wave function of the system, including all unoccupied states spanned by the plane wave basis set. Then, we compute the MP2 correlation energy using this set of orbitals. In the MP2 calculations, we separately use a Γ-centered 2 × 2 × 1 and 3 × 3 × 1 grid of k-points for the systems involving the slab. For the single water molecule in vacuum, by comparing results using cubic supercells with the length of the side of the supercell being 6 Å, 8 Å, 10 Å, or 12 Å, we find that using a supercell of 12 Å × 12 Å × 12 Å gives an MP2 correlation energy converged to within a few meV using just the Γ-point for sampling reciprocal space. Our results below indicate that overall, for a given ionic structure, our approach leads to MP2 adsorption energies converged to within a few tens of meV.

The VASP implementation of MP2 involves an auxiliary plane wave basis set for expanding the pseudized overlap charge density $\tilde{n}_{ij}(r) = \tilde{\psi}_i(r)\cdot\tilde{\psi}_j(r)$ using plane waves up to a kinetic energy cutoff of E_χ, here $\tilde{\psi}_i(r)$ indicating the pseudized orbital i.[24,25] To converge our results with respect to E_χ, we compute E_{MP2}^{corr} for the isolated molecule, slab in vacuum, and total slab and molecule system using a range of values for E_χ between 150 and 350 eV, and finally extrapolate the adsorption energy to infinite E_χ using the relation[24,25,39]

$$E_{MP2}^{corr}(E_\chi) = E_{MP2}^{corr}(E_\chi \to \infty) + AE_\chi^{-3/2} + BE_\chi^{-5/2} \quad (1)$$

where A and B are constants.

To find the equation of state of $SrTiO_3$ at each considered level of theory, we compute a series of (V,E) points at static conditions, where V is the volume and E is the total energy of the supercell. We then fit a third-order Birch−Murnaghan equation of state[40] to the data to find λ and K_0, the equilibrium lattice constant, and the bulk modulus at zero pressure, respectively. Unlike in our other MP2 calculations, to find the equation of state, we use a k-point sampling of 3 × 3 × 3, E_{cut} = 400 eV and E_χ = 250 eV. We assume the simple cubic perovskite structure for $SrTiO_3$ in all our bulk crystal calculations. For DFT, van der Waals DFT, hybrid-functional DFT, and Hartree−Fock, we find the minimum band gap from the computed set of quasiparticle eigenvalues.

The periodic slab geometry that we use for modeling the $SrTiO_3$ surface is shown in Figure 1. In the lateral direction, the repeating unit of the slab, extends to one full unit cell of the bulk-like (001) termination of the crystal, displaying either the TiO_2 or the SrO termination. We set the lateral lattice constant of the slab to the equilibrium bulk value found separately for

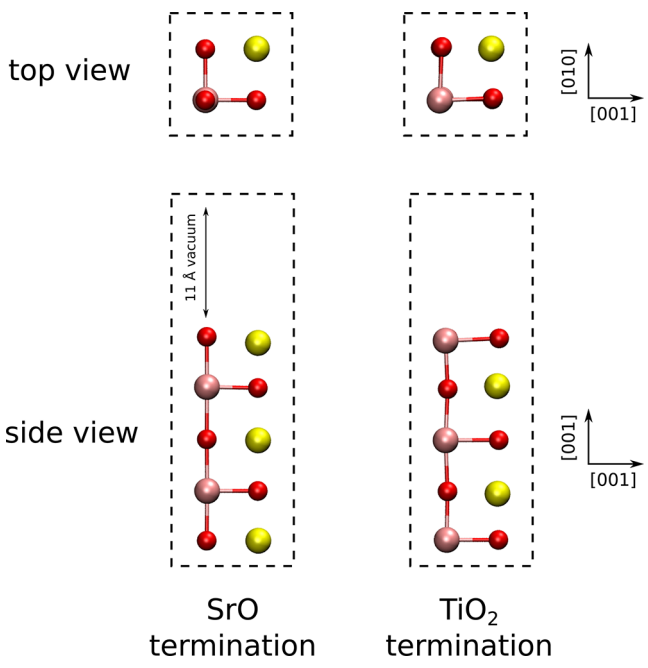

Figure 1. Supercell geometry for modeling the clean slab in vacuum, with the boundaries of the supercell shown by the dashed line. The SrO-terminated slab consists of 12 ions and the TiO_2-terminated slab of 13 ions. O is red, Ti is pink, and Sr is yellow.[41]

DOI: 10.1021/acs.jctc.7b00549
J. Chem. Theory Comput. 2017, 13, 6301−6307

each approach to the electronic structure problem and fix the bottom atomic layer. Our test calculations indicate that adsorption energies converged to within a few tens of meV can be obtained using a slab as thin as two full unit cells in the vertical direction (12 and 13 ions for the SrO and TiO_2 termination, respectively), and this is the size that we adopt for our calculations. A vacuum layer of 11 Å thickness gives us energies converged to within the limits given above. To obtain a vanishing surface dipole for the slab, the structure is made mirror-symmetrical with respect to the central atomic plane.

We find the equilibrium geometry of the isolated water molecule, the slab in vacuum, and the combined slab and molecule system using PBE, PBE-D3, PBE0, PBE0-D3, and optB86b by performing a conjugate-gradient geometry relaxation of the ionic positions until no total force larger than 0.01 eV/Å is present on any ion. To find the relaxed geometry of each slab system in vacuum, we applied small initial displacements to all except the fixed bottom layer of the slab prior to the relaxation. For each such case, we analyze for geometrical changes in the surface upon relaxation, as well as the surface energy and the minimum band gap. For the geometry relaxations of the combined slab and molecule system, we consider several different starting geometries regarding the water molecule with respect to the surface. From our results of the geometry optimizations and corresponding energies, we find the ground-state adsorption geometry for both molecular and dissociative adsorption on each surface termination for each treatment of exchange and correlation, the dissociative case being such that the molecule donates one proton to a surface O ion, and an OH fragment is left behind.[14] The adsorption energy is computed as

$$E_{ads} = E_{slab+H_2O} - (E_{slab} + E_{H_2O}) \quad (2)$$

where E_{slab+H_2O} is the energy of the relaxed slab and molecule system, E_{slab} is the energy of the slab in vacuum, and E_{H_2O} is the energy of the isolated water molecule. To find the adsorption energy within Hartree−Fock and MP2, we used the relaxed PBE0-D3 geometries and computed the Hartree−Fock and MP2 energies on these structures. Computing the MP2 correlation energy for the slab and molecule system at the highest auxiliary cutoff required approximately 70 h of runtime using a total of 1024 cores and approximately 2 TB of memory on a Cray XC40 supercomputer.

RESULTS

Bulk $SrTiO_3$ Crystal. We present the computed equilibrium properties of the $SrTiO_3$ crystal in comparison with experimental results from the literature in Table 1. The computed lattice constants are all within ∼1% of the experimental value, including the MP2 result of 3.94 Å. More variance is seen in the bulk modulus, with methods involving Hartree−Fock exact exchange predicting bulk moduli of 200 GPa and over, the other methods giving values much closer to experiment. Finally, the electronic band gap is not given in very good agreement with experiment by any of the applied methods, with GGA, dispersion-corrected GGA, and the van der Waals functional underestimating the gap, hybrid functionals overestimating it, and pure Hartree−Fock strongly overestimating it.

$SrTiO_3$ (001) in Vacuum. We present the surface energy and band gap of the slab system in Table 2. The computed surface energy of $SrTiO_3$ (001) ranges from approximately 1.1 to 1.7 J/m^2, with the dispersion-corrected calculations giving the highest surface energies and pure GGA the lowest energies. Whereas our PBE results are within the range of previously published PBE results[16,45] and our PBE0 results compare well with previous B3LYP results,[12] our PBE-D3 results for the surface energy are somewhat higher than recently published values.[16] The optB86b results for the surface energy are approximately midway between the extremes given by PBE and PBE0-D3. The band gaps of our slab systems are higher than in previous work,[16] which we find to be due to electronic confinement effects, based on comparison of the presented results with those from computations using a slab thicker by one unit cell of $SrTiO_3$.

The rumpling of our crystal surface is very similar to that found previously[16] and in similarly good agreement with experiment (Table 3). Relative displacements of the crystal planes upon relaxation from the bulk configuration are only in partial agreement with experiment, with experimental LEED and RHEED results in disagreement with each other, as noted previously (Table 4).[16,45]

Adsorption of H_2O onto $SrTiO_3$ (001). As described above, we find the MP2 correlation component to the adsorption energy by extrapolating to the infinite auxiliary basis set limit ($E_\chi \rightarrow \infty$). This is illustrated in Figure 2 for water adsorbed in the dissociative configuration on the SrO-terminated crystal. The adsorption energy of all four ionic configurations is given as a function of E_χ for both the 2 × 2 × 1 and the 3 × 3 × 1 k-grids in Table 5. The difference in the MP2 contribution to the adsorption energy at $E_\chi \rightarrow \infty$ between the two levels of k-point sampling is approximately 10 to 50 meV

Table 1. Equilibrium Lattice Parameter (λ), Bulk Modulus at Zero Pressure (B_0), and Minimum Band Gap (E_g) for the Bulk $SrTiO_3$ Crystal As Computed Here and As Found from Experiments Previously[a]

method	λ (Å)	B_0 (GPa)	E_g (eV)
PBE	3.95	175	2.0
PBE0	3.91	200	4.0
PBE-D3	3.92	183	2.0
PBE0-D3	3.88	210	4.1
optB86b	3.93	184	1.9
HF	3.92	220	11.7
MP2	3.94	176	-
experiment	3.90[42]	172[43]	3.3[44]

[a]Our static computational results are compared to experimental results at 300 K.

Table 2. Surface Energy of $SrTiO_3$ (001) in Vacuum, Given as the Average of the Surface Energies of the SrO and TiO_2-Terminated Slabs and the Band Gap of the Slab System for Each Termination, as Well as Results from Previous Studies

method	E_{surf} (eV/1 × 1)	E_{surf} (J/m^2)	E_g^{SrO} (eV)	$E_g^{TiO_2}$ (eV)
PBE	1.04	1.07	2.1	1.3
PBE0	1.15	1.21	3.9	3.4
PBE-D3	1.40	1.46	2.1	1.2
PBE0-D3	1.56	1.66	4.0	3.3
optB86b	1.36	1.41	1.6	1.1
PBE[16]	0.99	1.03	1.7	0.99
PBE[45]	1.23	1.28	-	-
PBE-D3[16]	1.23	1.28	1.7	0.94
B3LYP[12]	1.19	1.23	-	-

DOI: 10.1021/acs.jctc.7b00549
J. Chem. Theory Comput. 2017, 13, 6301−6307

Table 3. Rumpling (in Å) of the $SrTiO_3$ (001) Surface upon Relaxation As Computed Here and As Found in Previous Studies

method	SrO termination	TiO_2 termination
PBE	0.24	0.089
PBE0	0.22	0.087
PBE-D3	0.23	0.087
PBE0-D3	0.22	0.084
optB86b	0.24	0.075
PBE[16]	0.22	0.10
PBE-D3[16]	0.22	0.10
LEED[46]	0.16 ± 0.08	0.08 ± 0.08
RHEED[47]	0.16	0.10

for the four relaxed geometries. Using additional tests with a 4 × 4 × 1 grid of *k*-points, which could only be afforded with a slab no thicker than three atomic planes (7 ions), and using cutoff energies of E_{cut} = 300 eV and E_χ = 150 eV, we find the corresponding energy difference for the molecular adsorption mode on the SrO termination between the 4 × 4 × 1 and the 3 × 3 × 1 grids to be only 6 meV. In these test calculations, the difference in the corresponding energy between the 3 × 3 × 1 and 2 × 2 × 1 grids is 30 meV, in agreement with the calculations presented in Table 5. These results imply that the MP2 correlation component of the adsorption energy, as extrapolated to $E_\chi \to \infty$, is reasonably well converged with respect to the *k*-point sampling when using the 3 × 3 × 1 grid of *k*-points.

We present the final set of adsorption energies for the full range of methods employed in our calculations in Table 6. The corresponding geometries are illustrated in Figure 3, and the electron localization function (ELF)[48] for these is shown in Figure 4. We find the adsorption geometries to be very similar for all functionals used in the structural relaxations (PBE, PBE-D3, PBE0, PBE0-D3, optB86b), with O−H bond lengths differing at most by 0.03 Å between functionals. In Table 6, we also present the MP2 correlation contribution to the adsorption energy, alongside the corresponding contribution of the D3 dispersion correction and the nonlocal van der Waals correlation given by optB86b.

DISCUSSION

The MP2 result for the static adsorption energy of H_2O at an effective coverage of one monolayer is 0.9 eV on the SrO termination, for both modes of adsorption, and 0.6 and 0.9 eV on the TiO_2 termination for the dissociative and molecular modes, respectively. Comparing the DFT, hybrid DFT, van der Waals DFT, and Hartree−Fock results to MP2, we find PBE

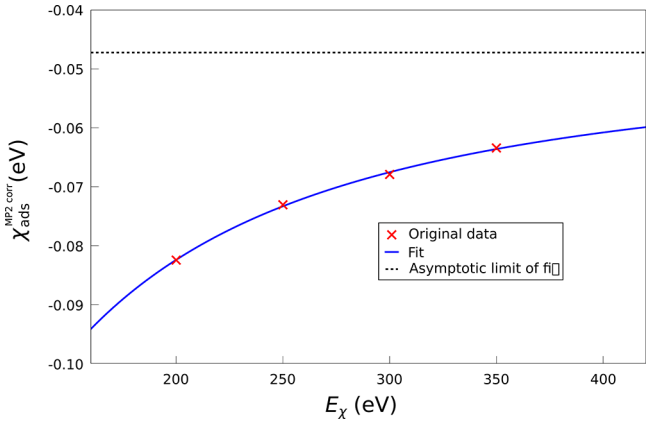

Figure 2. MP2 correlation energy component of the adsorption energy of water in the dissociative configuration on the SrO-terminated $SrTiO_3$ surface as a function of the cutoff energy for the auxiliary basis set (E_χ, see text) using a 2 × 2 × 1 grid of *k*-points. The data has been fitted to $E_{ads}^{MP2corr}(E_\chi) = E_{ads}^{MP2corr}(E_\chi \to \infty) + AE_\chi^{-3/2} + BE_\chi^{-5/2}$, where *A* and *B* are constants.

Table 5. Contribution of MP2 Correlation to the Adsorption Energy of Water on $SrTiO_3$ as a Function of the Cutoff Energy of the Auxiliary Basis Set (E_χ, see text) Given for the 2 × 2 × 1 (top) and the 3 × 3 × 1 (bottom) Sampling of the Brillouin Zone[a]

	SrO termination		TiO_2 termination	
E_χ	dissociative	molecular	dissociative	molecular
200	0.082	0.21	0.013	0.26
250	0.073	0.20	0.0092	0.25
300	0.068	0.20	0.0058	0.25
350	0.063	0.19	0.0025	0.24
∞	0.047	0.17	−0.016	0.23
	SrO termination		TiO_2 termination	
E_χ	dissociative	molecular	dissociative	molecular
150	0.14	0.27	−0.017	0.27
200	0.13	0.25	−0.021	0.26
250	0.12	0.24	−0.024	0.26
∞	0.092	0.22	−0.036	0.24

[a]Positive means a favorable energy of adsorption. All values are in eV.

Table 4. Change in Vertical Cation−Cation Distance (in Å) between the Outermost and Second-Outermost Planes (D_{12}) and the Second- and Third-Outermost Planes (D_{23}) of the $SrTiO_3$ (001) Surface upon Relaxation, As Computed Here and As Found from Previous Studies

	SrO termination		TiO_2 termination	
method	D_{12}	D_{23}	D_{12}	D_{23}
PBE	−0.27	0.091	−0.22	0.12
PBE0	−0.25	0.084	−0.20	0.11
PBE-D3	−0.25	0.090	−0.19	0.11
BE0-D3	−0.24	0.080	−0.18	0.10
optB86b	−0.26	0.084	−0.20	0.10
PBE[16]	−0.27	0.13	−0.23	0.16
PBE-D3[16]	−0.26	0.13	−0.21	0.15
LEED[46]	−0.20 ± 0.04	0.08 ± 0.04	0.04 ± 0.04	−0.04 ± 0.04
RHEED[47]	0.10	0.05	0.07	0.05

DOI: 10.1021/acs.jctc.7b00549
J. Chem. Theory Comput. 2017, 13, 6301−6307

Table 6. Final Results for the Energy of Adsorption (in eV) of H_2O onto $SrTiO_3$ (001) in the Most Favorable Dissociative and Molecular Configurations for Each Method and Surface Termination[a]

	SrO termination		TiO_2 termination	
method	dissociative	molecular	dissociative	molecular
PBE	0.93	0.92	0.61	0.80
PBE0	0.96	0.93	0.71	0.86
PBE-D3	1.1 (0.20)	1.1 (0.20)	0.77 (0.22)	0.98 (0.22)
PBE0-D3	1.1 (0.20)	1.1 (0.20)	0.87 (0.23)	1.0 (0.22)
optB86b	1.1 (0.45)	1.1 (0.45)	0.84 (0.59)	1.0 (0.56)
HF	0.78	0.67	0.62	0.64
MP2	0.87 (0.09)	0.89 (0.22)	0.59 (−0.04)	0.88 (0.24)

[a]The values in parentheses are the contribution of the D3 dispersion correction to the total adsorption energy for PBE-D3 and PBE0-D3, the nonlocal correlation for optB86b, and the MP2 correlation energy for MP2. The uncertainty due to finite sampling of the first Brillouin zone is estimated to be a few tens of meV for all methods.

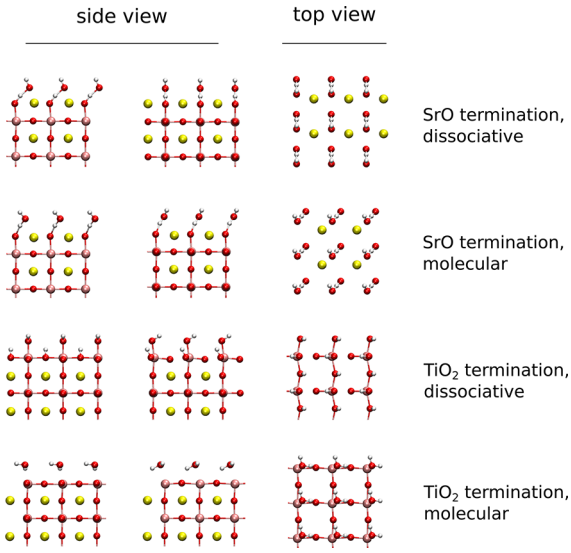

Figure 3. Most favorable adsorption geometry of H_2O on $SrTiO_3$ (001) in the molecular and the dissociative configuration for each surface termination as given by the PBE0-D3 functional. Three periodic repetitions of the supercell are shown in all dimensions. O is red, Ti is pink, Sr is yellow, and H is white.

and PBE0 to give the closest match with MP2, with a mean absolute difference of 0.05 and 0.07 eV, respectively. This is in contrast to the mean absolute differences of 0.18, 0.21, 0.20, and 0.15 eV for PBE-D3, PBE0-D3, optB86b, and HF as compared to the MP2 results, respectively. Despite only PBE and PBE0 showing good quantitative agreement with MP2, all the considered DFT and hybrid DFT methods are in qualitative agreement with MP2 regarding the preferred mode of adsorption, i.e., the dissociative and molecular modes being approximately degenerate on the SrO termination and the molecular mode being favored on the TiO_2 termination. Hartree−Fock, however, does not capture the same qualitative result, and instead favors the dissociative mode on the SrO termination and presents the two modes of adsorption as degenerate on the TiO_2 termination.

Considering that the D3 dispersion correction is an effective correction to the correlation energy, the method does not seem to correctly capture electron correlation in the present system.

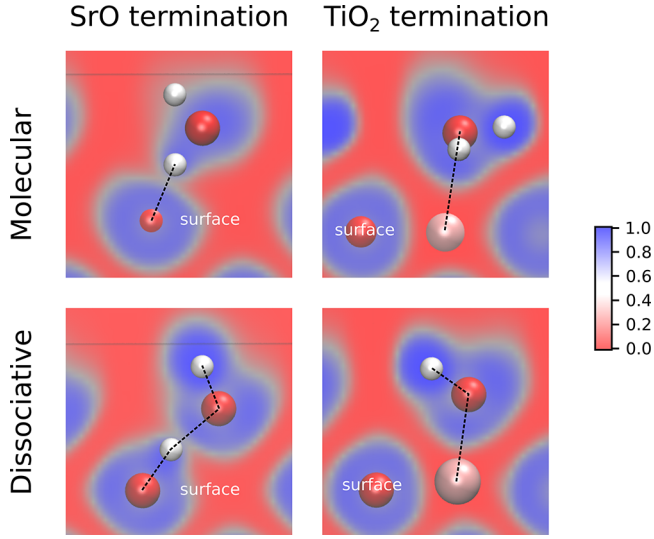

Figure 4. Electron localization function (ELF) plotted in two-dimensional slices through the most favorable adsorption geometries of H_2O on $SrTiO_3$ (001) as given by the PBE0-D3 functional. The dotted lines indicate which atoms of interest are in the same plane. The surface is indicated for each case.

This is seen by the fact that employing PBE-D3 or PBE0-D3 for treating exchange and correlation instead of pure PBE or PBE0 causes the adsorption energies to be overestimated by as much as 0.3 eV with respect to the MP2 results. The optB86b van der Waals functional gives adsorption energies very close to those given by PBE-D3 and PBE0-D3, in similar disagreement with MP2. This tendency of the D3 correction to overestimate adsorption energies with respect to higher-level quantum chemistry methods has been found earlier for the cases of water on MgF_2[49] and on LiH,[50] with also the optB86b functional displaying similar overestimation in the latter case. Furthermore, by inspecting the contribution of correlation energy to the adsorption energy, i.e., employing eq 2 for just the D3 energy, the nonlocal correlation of optB86b, or the MP2 correlation energy, we find that the D3 energy matches the MP2 correlation energy well for molecular adsorption states but disagrees for dissociative states (Table 6). It appears that the D3 method does not sufficiently differentiate between the two modes of adsorption, although the electronic structure does differ significantly between the two. The same is true of optB86b, with a fairly large margin to the MP2 results.

Examining the electronic structure through the ELF around the adsorbed molecule (Figure 4), we find that, for dissociative adsorption on the SrO termination, there exists a bond of weak covalent character between the surface-adsorbed proton and the OH fragment above. For the molecular configuration, there is a bond of weak covalent character between the surface oxygen and the H of the H_2O molecule above. In both of these cases, adsorption of the OH or H_2O to the surface thus appears to be due to hydrogen bonding as well as a low, but not negligible, degree of covalent interaction. For dissociative adsorption on the TiO_2 termination, we find an indication of covalent bonding between the OH fragment and the underlying Ti cation, but much less so in the molecular configuration. These results are in qualitative agreement with previous conclusions drawn from static DFT calculations on single-molecule adsorption.[16]

DOI: 10.1021/acs.jctc.7b00549
J. Chem. Theory Comput. 2017, 13, 6301−6307

Finally, we compare our MP2 results to experiment. From temperature-programmed desorption spectroscopy experiments,[51] it has been inferred[15] that the adsorption energy of water ranges from approximately 0.9 eV at the dilute coverage limit to 0.6 eV at an approximately 1 ML coverage on the TiO_2 termination of $SrTiO_3$ (001). Our corresponding MP2 results at 1 ML coverage are 0.6 and 0.9 eV in the dissociative and molecular states, respectively. While it was assumed in the experiment that water adsorbs in the molecular mode on the TiO_2-terminated $SrTiO_3$ (001) surface,[51] the actual mode of adsorption will always be a mixture of dissociated and molecular states, based purely on consideration of the configurational entropy related to a mixture of the two adsorption modes in the adsorbed water layer, considering for example the dissociated molecule as a defect in a layer of molecular water.[52] Taking this into account, our MP2 result of 0.6 eV for dissociative adsorption appears in agreement with the experimental result. We note, however, that our simulation is that of either a fully molecular or fully dissociated layer of water with a single unit cell as the repeating unit and is thus not directly comparable to experiment.

There is a qualitative consensus from experiment that water adsorbs predominantly in the dissociative mode on the SrO termination and mostly in the molecular mode on the TiO_2 termination.[13,51,53−55] Our MP2 result of an essentially degenerate adsorption energy for the two modes on the SrO termination is seemingly at odds with this result. However, at finite temperature, the entropic contribution to the free energy may well make the dissociative adsorption mode more favorable than the molecular mode, as the available number of microstates available to the adsorbed molecule after dissociation is likely higher than prior to dissociation. Yet again, the configurational entropy gain from having a mixture of dissociative and molecular adsorption states in an adsorbed layer of water instead of a uniformly molecular or dissociated one will favor a mixed mode of adsorption. It is not possible with our present model to draw strong conclusions on such a disordered layer of adsorbed water on $SrTiO_3$ (001).

CONCLUSIONS

Using periodic MP2 calculations, we find an adsorption energy of 0.9 eV for water on the SrO termination of $SrTiO_3$ (001) in both the molecular and dissociated states and 0.9 and 0.6 eV on the TiO_2 termination for the two modes, respectively. Apparent discrepancies with experiment, where the dissociative mode is found to dominate on the SrO-terminated surface, is suggested to be due to the neglect of entropic effects in the present approach. PBE and PBE0 reproduce these MP2 results to a reasonable accuracy. Adding on the D3 dispersion correction causes the energies of adsorption to significantly overestimate the MP2 results, and Hartree−Fock and optB86b van der Waals functional results likewise disagree with the MP2 results. The D3 dispersion correction nor the nonlocal electron correlation of the van der Waals functional differentiate between the molecular and dissociative adsorption states, whereas MP2 shows a significant difference in the contribution of electron correlation to the adsorption energy for the two cases. Overall, the PBE0 functional is our recommended choice for modeling the adsorption of water on $SrTiO_3$, as this functional gives adsorption energies in good agreement with MP2 and properties of the bulk crystal in good agreement with experiment. For higher coverages of water, the water−water interaction becomes important, and in this case the dispersion interaction and hence van der Waals functionals or the D3 correction may become preferrable options.

AUTHOR INFORMATION

Corresponding Author

*(E.H.) E-mail: eero.holmstrom@aalto.fi.

ORCID

E. Holmström: 0000-0002-4866-3730

A. S. Foster: 0000-0001-5371-5905

Notes

The authors declare no competing financial interest.

ACKNOWLEDGMENTS

We acknowledge financial support by the Academy of Finland through the Centres of Excellence Program (Project No. 251748). E.H. acknowledges financial support from the Emil Aaltonen foundation. We acknowledge that the results of this research have been achieved using the DECI resource Beskow based in Sweden at PDC/KTH with support from the PRACE aisbl. We also acknowledge CSC-IT Center for Science, Finland, for computational resources and application support.

REFERENCES

(1) Fujishima, A.; Honda, K. Electrochemical Photolysis of Water at a Semiconductor Electrode. *Nature* **1972**, *238*, 37−38.

(2) Wrighton, M. S.; Ellis, A. B.; Wolczanski, P. T.; Morse, D. L.; Abrahamson, H. B.; Ginley, D. S. Strontium Titanate Photoelectrodes: Efficient Photoassisted Electrolysis of Water at Zero Applied Potential. *J. Am. Chem. Soc.* **1976**, *98*, 2774−2779.

(3) Inoue, T.; Fujishima, A.; Konishi, S.; Honda, K. Photoelectrocatalytic reduction of carbon dioxide in aqueous suspensions of semiconductor powders. *Nature* **1979**, *277*, 637−638.

(4) Catlow, C. R. A.; Guo, Z. X.; Miskufova, M.; Shevlin, S. A.; Smith, A. G. H.; Sokol, A. A.; Walsh, A.; Wilson, D. J.; Woodley, S. M. Advances in computational studies of energy materials. *Philos. Trans. R. Soc., A* **2010**, *368*, 3379−3456.

(5) Brown, G. E.; Henrich, V. E.; Casey, W. H.; Clark, D. L.; Eggleston, C.; Felmy, A.; Goodman, D. W.; Grätzel, M.; Maciel, G.; McCarthy, M. I.; Nealson, K. H.; Sverjensky, D. A.; Toney, M. F.; Zachara, J. M. Metal Oxide Surfaces and Their Interactions with Aqueous Solutions and Microbial Organisms. *Chem. Rev.* **1999**, *99*, 77−174.

(6) Henderson, M. A. The interaction of water with solid surfaces: fundamental aspects revisited. *Surf. Sci. Rep.* **2002**, *46*, 1−308.

(7) Lindan, P. J. D.; Harrison, N. M.; Gillan, M. J. Mixed Dissociative and Molecular Adsorption of Water on the Rutile (110) Surface. *Phys. Rev. Lett.* **1998**, *80*, 762−765.

(8) Vittadini, A.; Selloni, A.; Rotzinger, F. P.; Grätzel, M. Structure and Energetics of Water Adsorbed at TiO_2 Anatase (101) and (001) Surfaces. *Phys. Rev. Lett.* **1998**, *81*, 2954−2957.

(9) Bandura, A. V.; Sykes, D. G.; Shapovalov, V.; Troung, T. N.; Kubicki, J. D.; Evarestov, R. A. Adsorption of Water on the TiO_2 (Rutile) (110) Surface: A Comparison of Periodic and Embedded Cluster Calculations. *J. Phys. Chem. B* **2004**, *108*, 7844−7853.

(10) Li, W.-K.; Gong, X.-Q.; Lu, G.; Selloni, A. Different Reactivities of TiO_2 Polymorphs: Comparative DFT Calculations of Water and Formic Acid Adsorption at Anatase and Brookite TiO_2 Surfaces. *J. Phys. Chem. C* **2008**, *112*, 6594−6596.

(11) Kumar, N.; Neogi, S.; Kent, P. R. C.; Bandura, A. V.; Kubicki, J. D.; Wesolowski, D. J.; Cole, D.; Sofo, J. O. Hydrogen Bonds and Vibrations of Water on (110) Rutile. *J. Phys. Chem. C* **2009**, *113*, 13732−13740.

(12) Evarestov, R. A.; Bandura, A. V.; Alexandrov, V. E. Adsorption of water on (001) surface of $SrTiO_3$ and $SrZrO_3$ cubic perovskites: Hybrid HF-DFT LCAO calculations. *Surf. Sci.* **2007**, *601*, 1844−1856.

DOI: 10.1021/acs.jctc.7b00549
J. Chem. Theory Comput. 2017, 13, 6301−6307

(13) Baniecki, J. D.; Ishii, M.; Kurihara, K.; Yamanaka, K.; Yano, T.; Shinozaki, K.; Imada, T.; Kobayashi, Y. Chemisorption of water and carbon dioxide on nanostructured $BaTiO_3$-$SrTiO_3$(001). *J. Appl. Phys.* **2009**, *106*, 054109.
(14) Guhl, H.; Miller, W.; Reuter, K. Water adsorption and dissociation on $SrTiO_3$(001) revisited: A density functional theory study. *Phys. Rev. B: Condens. Matter Mater. Phys.* **2010**, *81*, 155455.
(15) Hinojosa, B. B.; Van Cleve, T. V.; Asthagiri, A. A first-principles study of H_2O adsorption and dissociation on the $SrTiO_3$(100) surface. *Mol. Simul.* **2010**, *36*, 604−617.
(16) Holmström, E.; Spijker, P.; Foster, A. S. The interface of $SrTiO_3$ and H_2O from first-principles molecular dynamics. *Proc. R. Soc. London, Ser. A* **2016**, *472*, 20160293.
(17) Kumar, N.; Kent, P. R. C.; Wesolowski, D. J.; Kubicki, J. D. Modeling Water Adsorption on Rutile (110) Using van der Waals Density Functional and DFT+U Methods. *J. Phys. Chem. C* **2013**, *117*, 23638−23644.
(18) Liu, L.-M.; Zhang, C.; Thornton, G.; Michaelides, A. Structure and dynamics of liquid water on rutile TiO_2(110). *Phys. Rev. B: Condens. Matter Mater. Phys.* **2010**, *82*, 161415.
(19) Anchell, J. L.; Hess, A. C. H_2O Dissociation at Low-Coordinated Sites on $(MgO)_n$ Clusters, n = 4, 8. *J. Phys. Chem.* **1996**, *100*, 18317−18321.
(20) Stefanovich, E. V.; Truong, T. N. Ab initio study of water adsorption on TiO_2(110): molecular adsorption versus dissociative chemisorption. *Chem. Phys. Lett.* **1999**, *299*, 623−629.
(21) Sauer, J.; Horn, H.; Häser, M.; Ahlrichs, R. Formation of hydronium ions on Brønsted sites in zeolitic catalysts: a quantum-chemical ab initio study. *Chem. Phys. Lett.* **1990**, *173*, 26−32.
(22) Chen, M.; Straatsma, T. P.; Dixon, D. A. Molecular and Dissociative Adsorption of Water on $(TiO_2)_n$ Clusters, n = 1−4. *J. Phys. Chem. A* **2015**, *119*, 11406−11421.
(23) Kresse, G.; et al. Ab initio molecular dynamics for liquid metals. *Phys. Rev. B: Condens. Matter Mater. Phys.* **1993**, *47*, 558. Kresse, G.; Hafner, J. Ab initio molecular-dynamics simulation of the liquid-metal−amorphous-semiconductor transition in germanium. *Phys. Rev. B: Condens. Matter Mater. Phys.* **1994**, *49*, 14251. Kresse, G.; Furthmüller, J. Efficiency of ab-initio total energy calculations for metals and semiconductors using a plane-wave basis set. *Comput. Mater. Sci.* **1996**, *6*, 15. Kresse, G.; Furthmüller, J. Efficient iterative schemes for ab initio total-energy calculations using a plane-wave basis set. *Phys. Rev. B: Condens. Matter Mater. Phys.* **1996**, *54*, 11169.
(24) Marsman, M.; Grüneis, A.; Paier, J.; Kresse, G. Second-order M?ller-Plesset perturbation theory applied to extended systems. I. Within the projector-augmented-wave formalism using a plane wave basis set. *J. Chem. Phys.* **2009**, *130*, 184103.
(25) Grüneis, A.; Marsman, M.; Kresse, G. Second-order M?ller-Plesset perturbation theory applied to extended systems. II. Structural and energetic properties. *J. Chem. Phys.* **2010**, *133*, 074107.
(26) Martin, R. M. *Electronic Structure: Basic Theory and Practical Methods*; Cambridge University Press: Cambridge, U.K., 2008.
(27) Perdew, J. P.; Burke, K.; Ernzerhof, M. *Phys. Rev. Lett.* **1996**, *77*, 3865.
(28) Monkhorst, H. J.; Pack, J. D. *Phys. Rev. B* **1976**, *13*, 5188.
(29) Perdew, J. P.; Ernzerhof, M.; Burke, K. Rationale for mixing exact exchange with density functional approximations. *J. Chem. Phys.* **1996**, *105*, 9982.
(30) Adamo, C.; Barone, V. Toward reliable density functional methods without adjustable parameters: The PBE0 model. *J. Chem. Phys.* **1999**, *110*, 6158.
(31) Israelachvili, J. N. *Intermolecular and Surface Forces*; Academic Press: Burlington, VT, U.S.A., 2011.
(32) Dion, M.; Rydberg, H.; Schröder, E.; Langreth, D. C.; Lundqvist, B. I. Van der Waals Density Functional for General Geometries. *Phys. Rev. Lett.* **2004**, *92*, 246401.
(33) Klimes, J.; Bowler, D. R.; Michaelides, A. Chemical accuracy for the van der Waals density functional. *J. Phys.: Condens. Matter* **2010**, *22*, 022201.
(34) Klimes, J.; Bowler, D. R.; Michaelides, A. Van der Waals density functionals applied to solids. *Phys. Rev. B: Condens. Matter Mater. Phys.* **2011**, *83*, 195131.
(35) Roman-Perez, G.; Soler, J. M. Efficient Implementation of a van der Waals Density Functional: Application to Double-Wall Carbon Nanotubes. *Phys. Rev. Lett.* **2009**, *103*, 096102.
(36) Grimme, S.; Antony, J.; Ehrlich, S.; Krieg, H. A consistent and accurate ab initio parametrization of density functional dispersion correction (DFT-D) for the 94 elements H-Pu. *J. Chem. Phys.* **2010**, *132*, 154104.
(37) DFT-D3 web page at University of Bonn. http://www.thch.uni-bonn.de/tc/index.php?section=downloads&subsection=DFT-D3&lang=english (Accessed Jan 2017).
(38) Leach, A. R. *Molecular modelling: principles and applications*, 2nd ed.; Pearson Education: Harlow, U.K., 2001.
(39) Gulans, A. Towards numerically accurate many-body perturbation theory: Short-range correlation effects. *J. Chem. Phys.* **2014**, *141*, 164127.
(40) Birch, F. Equation of State and Thermodynamic Parameters of NaCl to 300 kbar in the High-Temperature Domain. *J. Geophys. Res.* **1986**, *91*, 4949−4954.
(41) Humphrey, W.; Dalke, A.; Schulten, K. VMD - Visual Molecular Dynamics. *J. Mol. Graphics* **1996**, *14*, 33−38.
(42) Abramov, Y. A.; Tsirelson, v. G.; Zavodnik, V. E.; Ivanov, S. A.; Brown, I. D. The Chemical Bond and Atomic Displacements in $SrTiO_3$ From X-ray Diffraction Analysis. *Acta Crystallogr., Sect. B: Struct. Sci.* **1995**, *51*, 942−951.
(43) Beattie, A. G.; Samara, G. A. Pressure Dependence of the Elastic Constants of $SrTiO_3$. *J. Appl. Phys.* **1971**, *42*, 2376.
(44) van Benthem, K.; Elsässer, C.; French, R. H. Bulk electronic structure of $SrTiO_3$: Experiment and theory. *J. Appl. Phys.* **2001**, *90*, 6156.
(45) Heifets, E.; Eglitis, R. I.; Kotomin, E. A.; Maier, J.; Borstel, G. Ab initio modeling of surface structure for $SrTiO_3$ perovskite crystals. *Phys. Rev. B: Condens. Matter Mater. Phys.* **2001**, *64*, 235417.
(46) Bickel, N.; Schmidt, G.; Heinz, K.; Müller, K. Ferroelectric Relaxation of the $SrTiO_3$(100) Surface. *Phys. Rev. Lett.* **1989**, *62*, 2009−2011.
(47) Hikita, T.; Hanada, T.; Kudo, M.; Kawai, M. Structure and electronic state of the TiO_2 and SrO terminated $SrTiO_3$(100) surfaces. *Surf. Sci.* **1993**, *287-288*, 377−381.
(48) Becke, A. D.; Edgecombe, K. E. A simple measure of electron localization in atomic and molecular systems. *J. Chem. Phys.* **1990**, *92*, 5397−5403.
(49) Kanaki, E.; Sansone, G.; Maschio, L.; Paulus, B. The effect of electron correlation on the adsorption of hydrogen fluoride and water on magnesium fluoride surfaces. *Phys. Chem. Chem. Phys.* **2015**, *17*, 18722.
(50) Tsatsoulis, T.; Hummel, F.; Usvyat, D.; Schütz, M.; Booth, G. H.; Binnie, S. S.; Gillan, M. J.; Alfè, D.; Michaelides, A.; Grüneis, A. A comparison between quantum chemistry and quantum Monte Carlo techniques for the adsorption of water on the (001) LiH surface. *J. Chem. Phys.* **2017**, *146*, 204108.
(51) Wang, L.-Q.; Ferris, K. F.; Herman, G. S. Interactions of H_2O with $SrTiO_3$(100) surfaces. *J. Vac. Sci. Technol., A* **2002**, *20*, 239−244.
(52) Ashcroft, N. W.; Mermin, N. D. *Solid State Physics*; Saunders College: Philadelphia, 1976.
(53) Lopez, A.; Heller, T.; Bitzer, T.; Chen, Q.; Richardson, N. V. The influence of sodium on the adsorption of water on $SrTiO_3$(100)-1 × 1 surfaces. *Surf. Sci.* **2001**, *494*, L811−L814.
(54) Iwahori, K.; Watanabe, S.; Kawai, M.; Kobayashi, K.; Yamada, H.; Matsushige, K. Effect of water adsorption on microscopic friction force on $SrTiO_3$ (001). *J. Appl. Phys.* **2003**, *93*, 3223−3227.
(55) Hussain, H.; Torrelles, X.; Rajput, P.; Nicotra, M.; Thornton, G.; Zegenhagen, J. A Quantitative Structural Investigation of the 0.1 wt % Nb-$SrTiO_3$(001)/H_2O Interface. *J. Phys. Chem. C* **2014**, *118*, 10980−10988.

DOI: 10.1021/acs.jctc.7b00549
J. Chem. Theory Comput. 2017, 13, 6301−6307